PHYSICAL REVIEW B VOLUME 9, NUMBER 5 1 MARCH 1974

Paramagnetic resonance of Cr^{3+} in tetragonal GeO_2[†]

David P. Madacsi,[*] M. Stapelbroek, and O. R. Gilliam

Department of Physics and Institute of Materials Science, The University of Connecticut, Storrs, Connecticut 06268

(Received 27 August 1973)

The ESR spectrum of Cr^{3+} in as-grown single crystals of tetragonal GeO_2 has been studied at X band at temperatures of 295 and 92 K. For the choice of magnetic axes $\vec{x} \| [001]$, $\vec{y} \| [1\bar{1}0]$, $\vec{z} \| [110]$, so chosen to minimize the ratio $|E/D|$, the spin-Hamiltonian parameters at 92 K are: $g_x = 1.979 \pm 0.001$, $g_y = 1.983 \pm 0.001$, $g_z = 1.977 \pm 0.001$; $|D| = 0.630 \pm 0.001$ and $|E| = 0.138 \pm 0.001$ in cm^{-1}; $A_x = 16.9 \pm 0.2$, $A_y = 16.0 \pm 0.2$, and $A_z = 16.0 \pm 0.2$ in units of 10^{-4} cm^{-1} for Cr^{53} hyperfine interaction; $A_{ax} = 2.1 \pm 0.1$, $A_{ay} = 1.9 \pm 0.1$, and $A_{az} = 1.9 \pm 0.1$ in units of 10^{-4} cm^{-1}, where this tensor represents the superhyperfine interaction with a Ge^{73} nucleus at one of the nearest-cation sites along the c axis. The zero-field splitting, represented by $\Delta_0 = 2(D^2 + 3E^2)^{1/2}$, is computed to be 1.348 ± 0.003 cm^{-1}. These results are compared with the results of previously reported studies of Cr^{3+} in the rutile-type hosts TiO_2 and SnO_2. The values of $|D|$, $|E|$, and the zero-field splitting Δ_0 are found to decrease in the order $SnO_2 \rightarrow TiO_2 \rightarrow GeO_2$. The core polarization and orbital contributions to the hyperfine field are also compared for these three hosts.

I. INTRODUCTION

Previous electron-spin-resonance (ESR) investigations of paramagnetic impurity ions in tetragonal GeO_2 have been limited to $S = \frac{1}{2}$ species. These have included the ions Mo^{5+} $(4d^1)$[1] and V^{4+} $(3d^1)$[2,3] in single crystals, and V^{4+} and Cu^{2+} $(3d^9)$ in polycrystalline samples.[4,5] Additional $S = \frac{1}{2}$ defects induced by radiation-damage mechanisms have been reported both in polycrystalline[6] and single-crystal[7] samples. In the isomorphic materials TiO_2 and SnO_2 many additional paramagnetic impurities have been studied, including the $S = \frac{3}{2}$ ions Cr^{3+} $3(d^3)$,[8,9] Mn^{4+} $(3d^3)$,[10] Ni^{3+} $(3d^7)$,[11] and Mo^{3+} $(4d^3)$[12] in TiO_2, and Cr^{3+}[13–15] and Mn^{4+}[16] in SnO_2. In the present paper we report the results of our investigation of the $S = \frac{3}{2}$ impurity Cr^{3+} in tetragonal GeO_2 single crystals, and compare these with the results of the previous studies of this ion in the TiO_2 and SnO_2 isomorphs. The well-known rutile structure is illustrated in Fig. 1. The unit cell belongs to the D_{4h}^{14} symmetry group and contains two inequivalent cation sites, with orthorhombic or D_{2h} point symmetry, which are related by a 90° rotation about the c axis. The Cr^{3+} impurity is substitutional at these sites. A distinction is noted in Fig. 1 between three types of nearest-neighbor Ge^{4+}-ion sites relative to the Cr^{3+} impurity.

II. EXPERIMENTAL DETAILS

Single crystals of tetragonal GeO_2 were grown from Na_2O and quartzlike GeO_2 starting materials by a flux method similar to that described by Swets.[17] Reddish single crystals of millimeter dimensions were obtained and were found by ESR to contain Cr^{3+}-, Fe^{3+}-, and Mn^{4+}-impurity ions. The last two of these will be discussed in subsequent publications. ESR spectra of Cr^{3+} were observed at 295 and 92 K with Varian E-3 and E-12 X-band spectrometers. All of the Cr^{3+} resonance lines were extremely narrow, even at 295 K, having widths of about 0.25–1.5 G between inflection points at both 295 and 92 K. Precise *in situ* orientation of the sample was obtained by means of a triple-axis goniometer head which permitted ± 15° rotation in two mutually orthogonal planes which were orthogonal to the horizontal plane in which full 360° rotation was possible.[18]

III. THEORY

The spin Hamiltonian which describes the ground-state energy levels of Cr^{3+} in a D_{2h} crystalline environment with an external field $\vec{H}$ is

$$\mathcal{H} = \mu_B \vec{H} \cdot \overleftrightarrow{g} \cdot \vec{S} + D\left[S_z^2 - \tfrac{1}{3}S(S+1)\right] + E(S_x^2 - S_y^2) + \vec{S} \cdot \overleftrightarrow{A}_{Cr} \cdot \vec{I}_{Cr} + \sum_{Ge} \vec{S} \cdot \overleftrightarrow{A}_{Ge} \cdot \vec{I}_{Ge} \,. \qquad (1)$$

Here, $\overleftrightarrow{A}_{Cr}$ and $\overleftrightarrow{A}_{Ge}$ are tensors which represent the hyperfine interaction with the Cr^{53} nucleus and superhyperfine (shf) interaction with neighboring Ge^{73} nuclei, respectively. The fourth-degree secular equation for the energy levels W at arbitrary orientations of the external field is[8]

$$0 = W^4 - W^2\left[\tfrac{5}{2}(g\mu_B H)^2 + 2D^2 + 6E^2\right] + W(g\mu_B H)^2(2D - 6D\cos^2\theta - 6E\sin^2\theta\cos 2\phi) + (D^2 + 3E^2)^2 + \tfrac{9}{16}(g\mu_B H)^4 + \tfrac{1}{2}(g\mu_B H)^2(D^2 - 6D^2\cos^2\theta + 9E^2\cos 2\theta + 12DE\sin^2\theta\cos 2\phi), \qquad (2)$$

where θ is the angle between the z axis and $\vec{H}$, and ϕ is the angle between the x axis and the projection of $\vec{H}$ onto the xy plane. The zero-field splitting is obtained from this equation by setting $H=0$, and is given by

$$\Delta_0 \equiv W_{1,2} - W_{3,4} = 2(D^2 + 3E^2)^{1/2}. \tag{3}$$

Solutions of the secular equation for $\vec{H}$ along principal axes are

$$\vec{H} \parallel \vec{z}: \quad \begin{aligned} W_{1,3} &= +\tfrac{1}{2}g_z\mu_B H_z \pm [(D+g_z\mu_B H_z)^2 + 3E^2]^{1/2}, \\ W_{2,4} &= -\tfrac{1}{2}g_z\mu_B H_z \pm [(D-g_z\mu_B H_z)^2 + 3E^2]^{1/2}, \end{aligned} \tag{4}$$

$$\vec{H} \parallel \vec{x}: \quad \begin{aligned} W_{1,3} &= +\tfrac{1}{2}g_x\mu_B H_x \pm [(D-\tfrac{1}{2}g_x\mu_B H_x)^2 + 3(E+\tfrac{1}{2}g_x\mu_B H_x)^2]^{1/2}, \\ W_{2,4} &= -\tfrac{1}{2}g_x\mu_B H_x \pm [(D+\tfrac{1}{2}g_x\mu_B H_x)^2 + 3(E-\tfrac{1}{2}g_x\mu_B H_x)^2]^{1/2}; \end{aligned} \tag{5}$$

$$\vec{H} \parallel \vec{y}: \quad \begin{aligned} W_{1,3} &= +\tfrac{1}{2}g_y\mu_B H_y \pm [(D-\tfrac{1}{2}g_y\mu_B H_y)^2 + 3(E-\tfrac{1}{2}g_y\mu_B H_y)^2]^{1/2}, \\ W_{2,4} &= -\tfrac{1}{2}g_y\mu_B H_y \pm [(D+\tfrac{1}{2}g_y\mu_B H_y)^2 + 3(E+\tfrac{1}{2}g_y\mu_B H_y)^2]^{1/2}. \end{aligned} \tag{6}$$

The secular equation also provides a means for checking the ratio E/D. When the splittings of the two Kramers doublets are equal, i.e., $W_2 - W_1 = W_4 - W_3$, this ratio is given by

$$E/D = (1 - 3\cos^2\theta)/3\sin^2\theta\cos 2\phi \, . \tag{7}$$

Hence, for a given choice of major axes, a knowledge of the coordinates (θ, ϕ) at which transitions between the two sets of levels occur at the same field value is sufficient to determine both the magnitude and the sign of the ratio E/D.

IV. RESULTS

A. Fine structure

Below 6 kG the ESR spectrum consists of two sets of fine-structure lines, each set attributed to Cr^{3+} impurities residing substitutionally at one of the two inequivalent cation sites which are related by a 90° rotation about the c axis. The two sets of lines coincide for the external field $\vec{H}$ along the c axis or along the a axis. The main two-line spectrum for each site is attributed to transitions between the split Zeeman levels of the $M_S = \pm\frac{1}{2}$ and $M_S = \pm\frac{3}{2}$ states. The lines have widths of about 0.25–1.5 G between inflection points both at 295 and 92 K and begin to saturate at less than a milliwatt of incident microwave power at 92 K.

The spin-Hamiltonian parameters g_i $(i = x, y, z)$, $|D|$, and $|E|$ were determined by fitting Eq. (2) to the observed spectra for $\vec{H}$ along principal magnetic axes. These axes, assigned according to the convention of minimizing the ratio $|E/D|$, are $\vec{x} \parallel [001]$, $\vec{y} \parallel [1\bar{1}0]$, $\vec{z} \parallel [110]$. The values obtained for g_i, $|D|$, and $|E|$ at temperatures of 295 and 92 K are given in Table I. The theoretical orientation dependence of the transitions was determined from solutions of Eq. (2) using these values. Figure 2 shows the observed and calculated angular dependences for rotation of the external field in the (001) plane and in the (110) plane. The energy levels, computed from Eqs. (4)–(6) using the spin-Hamiltonian parameters, are shown in Fig. 3 as a function of field strength along principal axes.

From the values determined for $|D|$ and $|E|$, the zero-field splitting according to Eq. (3) is $1.355 \pm 0.003\ \mathrm{cm^{-1}}$ at 295 K and $1.348 \pm 0.003\ \mathrm{cm^{-1}}$

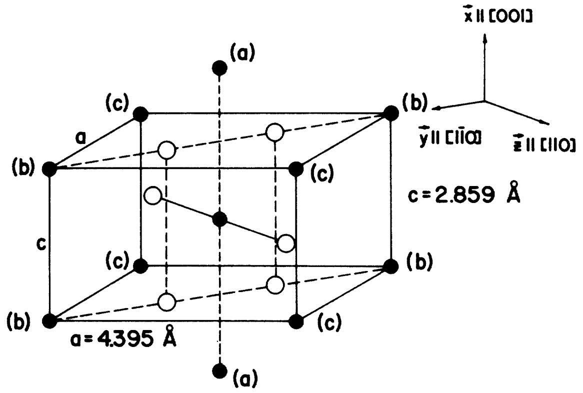

FIG. 1. Unit cell of tetragonal GeO_2 with the addition of neighboring (*a*) cations along the [001] direction. For interaction with an impurity located at the center of the unit cell, the (*a*) cations are inequivalent to the (*b*) cations which are in the diagonal plane containing four oxygens (open circles). The (*a*) and (*b*) cations are also inequivalent to the (*c*) cations which are coplanar with two oxygens.

TABLE I. Spin-Hamiltonian parameters for Cr^{3+} in tetragonal GeO_2 determined at X band at temperatures of 295 and 92 K. The values for $|D|$, $|E|$, and Δ_0, the zero-field splitting, are in units of cm^{-1}.

	$\lvert D\rvert$	$\lvert E\rvert$	g_x	g_y	g_z	Δ_0	$\lvert E/D\rvert$
295 K	0.634	0.137	1.979	1.983	1.978	1.355	0.216
92 K	0.630	0.138	1.979	1.983	1.977	1.348	0.219
Errors	±0.001	±0.001	±0.001	±0.001	±0.001	±0.003	±0.001

at 92 K. Comparison to results for Cr^{3+} in TiO_2 and SnO_2 indicates a decrease in zero-field splitting in the order $SnO_2 \rightarrow TiO_2 \rightarrow GeO_2$ as seen in Table II. From the angles $\phi = 90°$ and $\theta = 23°$ (or 67°), at which coincidence of the transitions due to Cr^{3+} at one site (or the other) occurred (see Fig. 2), the ratio E/D was calculated. This ratio was used to distinguish which transitions corresponded to a particular Cr^{3+} site, and which corresponded to the second site related to the first by a 90° rotation about the c axis. Utilizing Eq. (7), the choice $\phi = 90°$, $\theta = 23°$ gave a value E/D greater than unity, while the choice $\phi = 90°$, $\theta = 67°$ gave a value $E/D = -0.213$. This latter value is in agreement with the experimentally determined ratio $|E/D| = 0.217$. Hence E and D are opposite in sign for the given choice of axes.

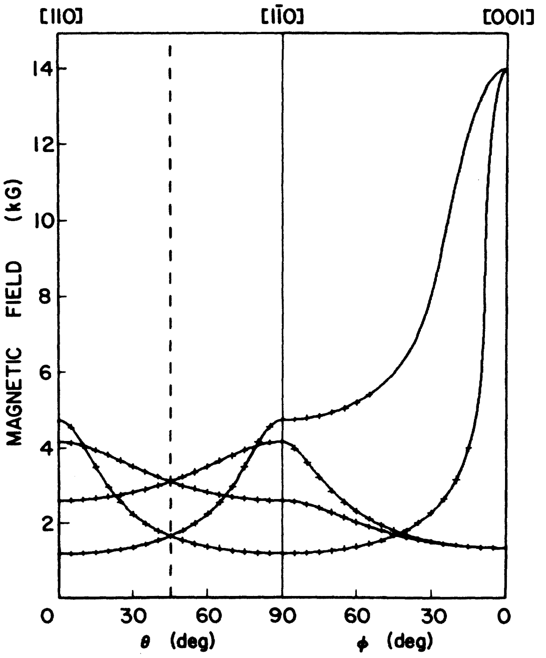

FIG. 2. Variation of the ESR spectrum of Cr^{3+} in GeO_2 with rotation of $\vec{H}$ in the (001) and (110) planes. The microwave frequency is 9.2 GHz. Solid curves represent theoretical calculations based on measured parameters. Crosses represent observed resonances. Only transitions between the terms of Kramers doublets are plotted.

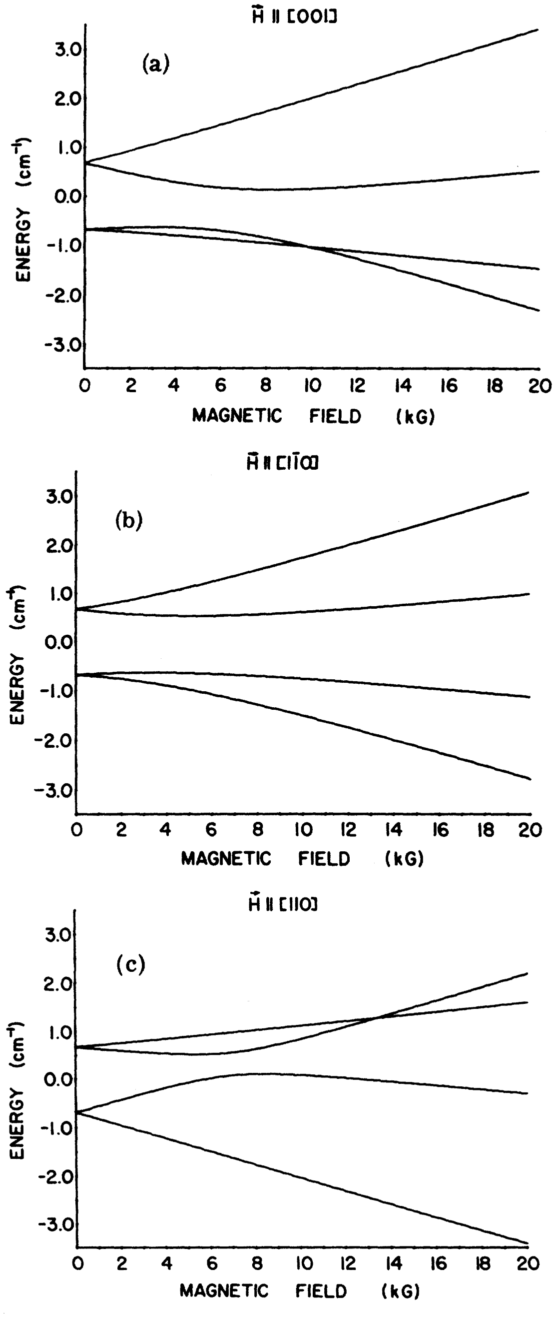

FIG. 3. Energy levels of Cr^{3+} substitutional at cation sites in tetragonal GeO_2 for $\vec{H}$ along principal axes: (a) $\vec{H} \parallel [001]$, (b) $\vec{H} \parallel [1\bar{1}0]$, and (c) $\vec{H} \parallel [110]$.

TABLE II. Spin-Hamiltonian parameters for Cr^{3+} substitutional at cation sites in rutilelike hosts. The values for $|D|$, $|E|$, and Δ_0, the zero-field splitting, are in units of cm^{-1}.

Host	T (K)	g_{av}	$\|D\|$	$\|E\|$	Δ_0	$\|E/D\|$	Ref.
SnO_2	≈295	1.975	0.684	0.185	1.511	0.271	14
SnO_2	4.2	1.973	0.658	0.177	1.451	0.269	15
TiO_2	77	1.97	0.68	0.14	1.44	0.21	9
GeO_2	295	1.980	0.634	0.137	1.355	0.216	This work
GeO_2	92	1.980	0.630	0.138	1.348	0.219	This work

B. Hyperfine structure

Each fine-structure line exhibits a hyperfine structure consisting of four equally spaced lines centered about it. The hyperfine lines have summed intensities about 10% of the intensity of the main line and result from the 9.43% abundant Cr^{53} isotope with $I = \frac{3}{2}$. The over-all splitting of the hyperfine lines is 52–55 G depending on crystal orientation in the external field. The Cr^{53} hyperfine tensor components for the Cr^{3+} ion in GeO_2, TiO_2, and SnO_2 are given in Table III. Because the spin resonances are especially narrow for the GeO_2 host, the hyperfine lines are well resolved by ESR and the small anisotropy in the hyperfine interaction is measurable.

C. Superhyperfine structure

The only stable isotope of germanium which has a nonzero nuclear moment is the 7.76% abundant Ge^{73}, which has a spin $I_{Ge} = \frac{9}{2}$. The interaction between the unpaired electronic moments of Cr^{3+} impurities and the nuclear moments of neighboring Ge^{73} nuclei results in a shf structure. Ten equally spaced shf lines are observed centered about each fine-structure line with an over-all splitting ranging from about 18.5 to 20.6 G. These lines are at least partially resolved for all orientations with respect to $\vec{H}$, and are shown in Fig. 4 for $\vec{H} \parallel [110]$. They are attributed to interaction with Ge^{73} nuclei located at nearest-neighbor (a) cation sites along the [001] direction. A less-well-resolved structure observed alongside the main line in Fig. 4 is attributed to shf interaction with Ge^{73} nuclei at (b) and (c) cation sites (see Fig. 1). Measurement of the over-all splitting of these lines permitted a determination of the maximum value for the corresponding shf interaction constant. Table IV summarizes the shf interaction constants for the various cation sites for Cr^{3+} and V^{4+} in the three hosts SnO_2, TiO_2, and GeO_2. Superhyperfine interactions involving individual Cr^{3+} ions and Ge^{73} nuclei at two or more equivalent neighboring sites were not observed because of their significantly lower probabilities.

TABLE III. Hyperfine-tensor components for Cr^{3+} substitutional at cation sites in rutilelike hosts. Units are 10^{-4} cm^{-1}.

Host	A_x	A_y	A_z	Ref.
SnO_2	17.5	16.7	16.6	15
TiO_2	15	15	15	9
GeO_2	16.9	16.0	16.0	This work

V. DISCUSSION

The trivalent chromium impurity has now been studied by ESR in single crystals of the three rutile-type hosts SnO_2, TiO_2, and GeO_2. Differences as well as similarities in the ESR spectra and related parameters should be interpretable to some extent in terms of the host lattices. As might be expected,

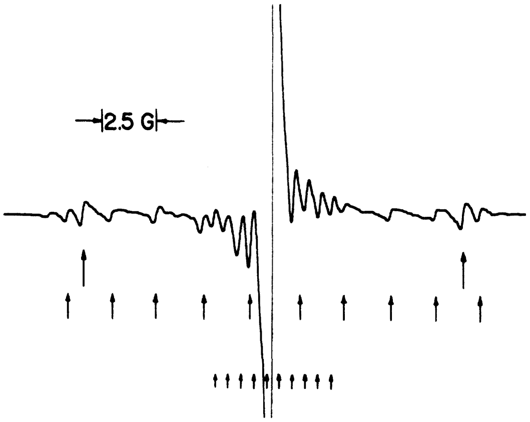

FIG. 4. Low-field fine-structure line of Cr^{3+} in GeO_2 with $\vec{H} \parallel [110]$ showing associated hyperfine and superhyperfine structure. The two lines separated by about 27 G (identified by long arrows) are two of the four Cr^{53} hyperfine lines (the other two lie outside the field range displayed). The ten equally spaced lines with an over-all splitting of about 19 G (identified by intermediate-sized arrows) are attributed to the (a)-cation Ge^{73} shf interaction. The ten equally spaced lines with an over-all splitting of about 5 G (identified by short arrows) are attributed to unresolved (b)- and (c)-cation Ge^{73} shf interactions.

TABLE IV. Superhyperfine-tensor components for Cr^{3+} and V^{4+} ions substitutional at cation sites in rutilelike hosts. Units are 10^{-4} cm^{-1}.

System	Cation	$A[001]$	$A[1\bar{1}0]$	$A[110]$	Ref.
$SnO_2:Cr^{3+}$	(*a*)	33.8	31.7	31.1	15
	(*b*)	6.1	6.1	5.2	
	(*c*)	6.6	6.7	7.5	
$TiO_2:Cr^{3+}$	(*a*), (*b*), (*c*)	unresolved	unresolved	unresolved	9
$GeO_2:Cr^{3+}$	(*a*)	2.1	1.9	1.9	This work
	(*b*), (*c*)	0.4(5)	unresolved	0.5(5)	
$SnO_2:V^{4+}$	(*a*)	153.3	150	149.9	19
	(*b*)	25	25	25	
$TiO_2:V^{4+}$	(*a*)	2.1	1.8	1.8	20
$GeO_2:V^{4+}$	(*a*)	8.8	8.4	8.3	3
	(*b*)	1.8	1.8	1.8	

the splitting of the ground-state energy levels by an external field and the orientation dependence of the transitions between these levels have the same general features for the three hosts. Comparison also indicates that there are variations in g_i for the three hosts which are greater than experimental error, and that $|D|$ and $|E|$ depend on the lattice spacing. The general tendency is an increase in both $|D|$ and $|E|$ in the host sequence $GeO_2 \rightarrow TiO_2 \rightarrow SnO_2$, which is the order of increasing lattice spacing as given in Table V. The zero-field splitting Δ_0 also increases in this order. This general tendency of increasing $|D|$, $|E|$, and Δ_0 with increasing lattice spacing is also observed in the temperature dependence of these parameters (see Table II) for the individual hosts SnO_2 and GeO_2 (since lattice dimensions increase with temperature).

The ratio E/D for Cr^{3+} in tetragonal GeO_2 is found to be negative for the given choice of axes, in agreement with the results reported for Cr^{3+} in TiO_2[9] and SnO_2[13] for which the signs of both E and D were determined from intensity measurements at 4.2 and 1.5 K. For both of these hosts E was determined to be positive and D negative. Because of the similarities of the three rutile-type hosts, and because of the regularities in the variations of the Cr^{3+} spin-Hamiltonian parameters among them, it is likely that the sign of E is positive and D is negative for Cr^{3+} in the GeO_2 host also. The minimum ratio $|E/D|$, a measure of the rhombic character at the Cr^{3+} impurity site, is greatest for SnO_2 and has approximately equal values for TiO_2 and GeO_2.

TABLE V. Lattice dimensions[a] in angstrom units for rutile-type crystals.

Lattice dimension	GeO_2	TiO_2	SnO_2
a_0	4.3975	4.5941	4.7380
c_0	2.8625	2.9589	3.1865

[a] W. H. Baur and A. A. Khan, Acta Crystallog B <u>27</u>, 2133 (1971).

The contact hyperfine interaction exhibits variations among the three hosts which exceed experimental errors. These differences can be understood by considering the principal contributions to the hyperfine field, viz., the orbital hyperfine field and the core-polarization hyperfine field (the dipole contribution is taken to be negligible). The former is given by[21]

$$H^{\rm hf}_{\rm orb} = +2.0023\mu_B \langle r^{-3}\rangle \Delta g_L , \qquad (8)$$

where Δg_L is the orbital contribution to the g shift. Since the ground state of Cr^{3+} is orbitally nondegenerate, the observed g shifts can be assumed completely orbital in origin. The difference between the experimentally measured hyperfine field and the orbital field is then attributed to the core-polarization hyperfine field

$$H^{\rm hf}_{\rm cp} = -A/g_I\mu_N - H^{\rm hf}_{\rm orb} . \qquad (9)$$

For $3d^5$ ions as well as for $3d^8$ ions, the core-polarization field has been observed to be independent of lattice spacing, and to remain constant for isoelectronic impurities in a given host.[21,22] The orbital field has also been found to be independent of lattice spacing for $3d^5$ ions in sixfold oxygen coordination, for which $H^{\rm hf}_{\rm orb}$ is a small fraction of $H^{\rm hf}_{\rm total}$. For $3d^8$ ions, however, $H^{\rm hf}_{\rm orb}$ is a significant fraction of the total hyperfine field, and it is not independent of lattice spacing.

For $3d^3$ ions, the orbital hyperfine field is a relatively small part of the total hyperfine field, but it is larger than that for $3d^5$ ions, and it does vary with lattice spacing as well as among isoelectronic impurities in a given host. The core-polarization hyperfine field, however, has been found to remain constant for isoelectronic $3d^3$ impurities in a host.[23] In addition, Rhein[15] has recently shown

TABLE VI. Comparison of core-polarization and orbital contributions to the total hyperfine field of Cr^{3+} ions substitutional at cation sites in the rutilelike hosts SnO_2, TiO_2, and GeO_2. Fields are in kilogauss.

Host	Field direction	Δg	H^{hf}_{total}	H^{hf}_{orb}	H^{hf}_{cp}	Maximum estimated error	Ref.
SnO_2	$\vec{H} \parallel [001]$	−0.029	−229.5	−14.4	−215.1	±2.0	15
	$\vec{H} \parallel [1\bar{1}0]$	−0.028	−219.0	−13.9	−205.1	±2.0	
	$\vec{H} \parallel [110]$	−0.031	−217.7	−15.3	−202.4	±2.0	
GeO_2	$\vec{H} \parallel [001]$	−0.023	−221.6[a]	−11.4	−210.2	±2.0	This work
	$\vec{H} \parallel [1\bar{1}0]$	−0.019	−209.8[a]	−9.4	−200.4	±2.0	
	$\vec{H} \parallel [110]$	−0.025	−209.8[a]	−12.4	−197.4	±2.0	
TiO_2	Average	−0.03 ± 0.01	−197 ± 30[a]	−15 ± 5	−182 ± 35		9

[a] It is assumed that the total hyperfine field for Cr^{3+} in GeO_2 and TiO_2 has the same sign as reported for the hosts SnO_2, Al_2O_3, and MgO (Ref. 15).

it to be constant to within about $\frac{1}{2}\%$ in a comparison of results for Cr^{3+} in MgO, Al_2O_3, and SnO_2. The present results add empirical evidence for the constancy of the core polarization for this $3d^3$ ion as the lattice spacing is varied for a unique (locally distorted) crystal symmetry.

Table VI symmarizes the hyperfine-field contributions for Cr^{3+} in the three rutile-type hosts SnO_2, TiO_2, and GeO_2. It is assumed that the total hyperfine field for Cr^{3+} in GeO_2 and TiO_2 has the same sign as reported for the hosts SnO_2, Al_2O_3, and MgO.[15] The g shift is anisotropic, varies with host, and leads to a value for the orbital hyperfine field which ranges from about −9 to −15 kG, based on the free-ion value of 3.95 atomic units for $\langle 1/r^3 \rangle$ as calculated by Freeman and Watson.[24] For TiO_2 the uncertainties in Δg and A lead to a large uncertainty in the core-polarization field, so that its value overlaps those for SnO_2 and GeO_2. However, the uncertainties in Δg_i and A_i $(i = x, y, z)$ for SnO_2 and GeO_2 are small, and the values of the core-polarization hyperfine field computed along the principal axes for these hosts do not overlap. The deviation in H^{hf}_{cp} for Cr^{3+} in the two hosts is the same for the three directions, about 5 kG. This difference, amounting to a few percent of H^{hf}_{cp}, may be due to the fact that quadrupole effects were neglected in determining the total hyperfine field in the present work on GeO_2, whereas the quadrupole interaction was measured in the electron-nuclear-double-resonance (ENDOR) studies of Cr^{3+} in SnO_2.[15] Since the quadrupole field for Cr^{3+} in SnO_2 is of the order of 1% of the total hyperfine field, it will be necessary to measure the quadrupole interaction for Cr^{3+} in GeO_2 before this difference can be resolved. Hence an ENDOR study of this system appears warranted.

TABLE VII. Comparison of ratios of cation-orbital admixture coefficients, $|\mu_a/\mu_b|$ for Cr^{3+} and V^{4+} ions substitutional at cation sites in SnO_2 and GeO_2. Hyperfine-interaction constants are in units of 10^{-4} cm^{-1}.

System	A_a	A_b	$\lvert\mu_a/\mu_b\rvert = (A_a/2A_b)^{1/2}$	Ref.
$SnO_2 : V^{4+}$	151.2	25	1.7	19
$SnO_2 : Cr^{3+}$	32.2	5.8	1.7	15
$GeO_2 : V^{4+}$	8.5	1.8	1.5	3
$GeO_2 : Cr^{3+}$	2.0	0.5	1.4	This work

An ENDOR study would also be useful in further resolving the shf interactions of the Cr^{3+} impurity with the (b) and (c) cations. However, the resolution which has been obtained for the (a)-cation shf structure as well as the partial resolution of the (b)-cation shf structure is sufficient to provide some information about the relative delocalization of the Cr^{3+} unpaired spin onto the (a) and (b) cations. The isotropic part of the shf interaction is related to the unpaired-spin density at the ligand nucleus $\rho(\vec{r}_n)$ by

$$A = \tfrac{1}{3}(A_x + A_y + A_z) = \tfrac{8}{3}\pi g_e \mu_B g_I \mu_N \rho(\vec{r}_n). \qquad (10)$$

We will approximate the unpaired-spin density at cations of type (a) and type (b), respectively, by

$$\rho(\vec{r}_a) \simeq \tfrac{1}{2} N^{-1} \mu_a^2 \, |S(0)|^2 \qquad (11)$$

and

$$\rho(\vec{r}_b) \simeq \tfrac{1}{4} N^{-1} \mu_b^2 \, |S(0)|^2 \, , \qquad (12)$$

where N is a normalization factor, μ_a and μ_b are coefficients describing the admixture of (a) and (b) cation orbitals, and $S(0)$ is the value of the cation S orbital at the nucleus. A knowledge of the normalization factor N is required for a determination of the absolute magnitudes of μ_a and μ_b, and can be obtained in cases of nd^1 configurations such as for V^{4+}.[3,25] For the present example of a $3d^3$ configuration, it is possible to obtain the relative magnitudes $|\mu_a/\mu_b|$ independent of a knowledge of N. Equations (10)–(12) combine to give

$$|\mu_a/\mu_b| = |A_a/2A_b|^{1/2} . \tag{13}$$

Based on this relationship, it is found that within the accuracy of our approximation this ratio is about the same for Cr^{3+} as for V^{4+} in both SnO_2 and GeO_2, and is slightly greater in SnO_2. The values obtained for this ratio are summarized in Table VII.

ACKNOWLEDGMENTS

We wish to thank Dr. E. Kostiner and H. B. Van Rees for assistance in the preparation of single crystals for this study. We also acknowledge helpful discussions with Dr. R. H. Bartram. The computational portions of this investigation were performed at the University of Connecticut Computer Center.

---

†Supported in part by the University of Connecticut Research Foundation and by the U. S. Public Health Service, N. I. D. R. Grant No. DE-03425.

*Present address: Dept. of Physics, The Pennsylvania State University, The Shenango Valley Campus, Sharon, Pa. 16146.

[1] T. Purcell and R. A. Weeks, Phys. Lett. A 38, 473 (1972).

[2] D. P. Madacsi and O. R. Gilliam, Phys. Lett. A 41, 63 (1972).

[3] D. P. Madacsi, R. H. Bartram, and O. R. Gilliam, Phys. Rev. B 7, 1817 (1973).

[4] I. Siegel, Phys. Rev. 134, A193 (1964).

[5] I. Siegel and J. A. Lorenc, J. Chem. Phys. 45, 2315 (1966).

[6] R. A. Weeks and T. Purcell, J. Chem. Phys. 43, 483 (1965).

[7] D. P. Madacsi and O. R. Gilliam, Bull. Am. Phys. Soc. 18, 467 (1973).

[8] H. J. Gerritsen, S. E. Harrison, H. R. Lewis, and J. P. Wittke, Phys. Rev. Lett. 2, 153 (1959).

[9] H. J. Gerritsen, S. E. Harrison, and H. R. Lewis, J. Appl. Phys. 31, 1566 (1960).

[10] H. G. Andresen, Phys. Rev. 120, 1606 (1960).

[11] H. J. Gerritsen and E. S. Sabisky, Phys. Rev. 125, 1853 (1962).

[12] W. D. Ohlsen, Phys. Rev. B 7, 4058 (1973).

[13] W. H. From, Phys. Rev. 131, 961 (1963).

[14] S. L. Hou, R. W. Summitt and R. F. Tucker, Phys. Rev. 154, 258 (1967).

[15] W. Rhein, Z. Naturforsch. A 27, 741 (1972).

[16] W. H. From, P. B. Dorain, and C. Kikuchi, Bull. Am. Phys. Soc. 9, 244 (1964).

[17] D. E. Swets, J. Crystal Growth 8, 311 (1971).

[18] M. Batley, R. Bromley, B. E. Merz, and W. Orr, Rev. Sci. Instrum. 43, 425 (1972).

[19] C. Kikuchi, I. Chen, W. H. From, and P. B. Dorain, J. Chem. Phys. 42, 181 (1965).

[20] H. J. Gerritsen and H. R. Lewis, Phys. Rev. 119, 1010 (1960).

[21] S. Geschwind, in *Hyperfine Interactions*, edited by A. J. Freeman and R. B. Frankel (Academic, London, 1967), Chap. 6.

[22] A. Abragam and B. Bleaney, *Electron Paramagnetic Resonance of Transition Ions* (Clarendon, Oxford, 1970).

[23] N. Laurance and J. Lambe, Phys. Rev. 132, 1029 (1963).

[24] A. J. Freeman and R. E. Watson, *Magnetism*, edited by G. T. Rado and H. Suhl (Academic, New York, 1965), Vol. IIA, Appendix B.

[25] T. Shimizu, J. Phys. Soc. Jap. 23, 848 (1967).